

RIGA TECHNICAL UNIVERSITY
Faculty of Electronics and Telecommunications
Institute of Radio Electronics

Kaspars OZOLS
Student of the Doctoral study program "Electronics"

**ASYNCHRONOUS DATA ACQUISITION OF
ELECTROENCEPHALOGRAM SIGNALS**

Summary of the Doctoral Thesis

Scientific Supervisor
Senior Researcher, *Dr.sc.comp.*
MODRIS GREITANS

RTU Press
Riga 2017

Ozols K. ASYNCHRONOUS DATA
ACQUISITION of ELECTRO-
ENCEPHALOGRAM SIGNALS.
Summary of the Doctoral Thesis.
– R.:RTU Press, 2017. -34 p

Printed according to the decision of RTU
Promotion Council “RTU P-08” of
16 March 2017, Minutes No. 39

ISBN 978-9934-10-956-0

**DOCTORAL THESIS
PROPOSED TO RIGA TECHNICAL UNIVERSITY FOR THE PROMOTION TO THE
SCIENTIFFIC DEGREE OF DOCTOR OF ENGINEERING SCIENCES
(ELECTRONICS)**

To be granted the scientific degree of Doctor of Engineering Sciences, the present Doctoral Thesis has been submitted for the defence at the open meeting of RTU Promotion Council “RTU P-08” on 16 June 2017 at the Faculty of Electronics and Telecommunications of Riga Technical University, 12 Azenes Street, Room 120.

OFFICIAL REVIEWERS

Professor *Dr. habil. sc. ing.* Andris Ozols
Riga Technical University, Latvia

Senior Researcher *Dr. math.* Maris Alberts
University of Latvia, Latvia

Associated Professor *Dr. sc. ing* Dainius Udris
Vilnius Gediminas Technical University, Lithuania

DECLARATION OF ACADEMIC INTEGRITY

I hereby declare that the Doctoral Thesis submitted for the review to Riga Technical University for the promotion to the scientific degree of Doctor of Engineering Sciences (Electronics) is my own. I confirm that this Doctoral Thesis had not been submitted to any other university for the promotion to a scientific degree.

Kaspars Ozols(Signature)

Date:

The doctoral thesis is written in English, contains introduction, 5 chapters, conclusions, references, 12 appendices, an index, 72 figures and 13 tables, 174 pages in total. The list of references consists of 183 titles.

TABLE OF CONTENTS

ABBREVIATIONS.	5
NOMENCLATURE	6
GENERAL DESCRIPTION OF THE WORK	7
The Urgency of Subject Matter	7
The Objective of the Work	8
The Methodology of Research	8
Scientific Novelty and Main Results	8
Thesis Statements to Be Defended	9
Practical Value and Approbation	9
Structure of the Thesis	10
1. BACKGROUND AND RELATED WORK	11
1.1 Electroencephalogram Signals	11
1.2 Analogue-to-Digital Converters	11
1.3 Conclusions	13
2. ASYNCHRONOUS SIGMA-DELTA MODULATOR	14
2.1 Signal Encoding	14
2.2 Signal Recovery	15
2.3 Advantages and Disadvantages	17
2.4 Conclusions	17
3. AMPLITUDE ADAPTIVE ASYNCHRONOUS SIGMA-DELTA MODULATOR	18
3.1 AA-ASDM with additional envelope encoding	19
3.2 AA-ASDM without additional envelope encoding	19
3.3 Conclusions	21
4. EXPERIMENTAL RESEARCH	22
4.1 Simulations	22
4.1.1 Asynchronous Sigma-Delta Modulator	22
4.1.2 AA-ASDM with additional envelope encoding	22
4.1.3 AA-ASDM without additional envelope encoding	23
4.2 Modeling	25
4.2.1 Asynchronous Sigma-Delta Modulator	25
4.2.2 AA-ASDM without additional envelope encoding	25
4.3 Practical Implementations	28
4.4 Conclusions	30
5. CONCLUSIONS	31
BIBLIOGRAPHY	32

ABBREVIATIONS

AA-ASDM – *amplitude adaptive asynchronous sigma-delta modulator*
AA-ASDM1 – *AA-ASDM with additional envelope encoding*
AA-ASDM2 – *AA-ASDM without additional envelope encoding*
ADC – *analog-to-digital converter*
ASDM – *asynchronous sigma-delta modulator*
ATS460 – *waveform digitizer* BCI – *brain computer interface*
DC – *direct current*
ECG – *electrocardiogram*
EEG – *electroencephalogram*
EMG – *electromyogram*
EMI – *electromagnetic interference*
ENOB – *effective number Of bits*
EOG – *electrooculogram*
HDR – *high dynamic range*
LC ADC – *level crossing ADC*
OOK – *on-off keying*
PC – *personal computer*
PCB – *printed circuit board*
SAR – *successive approximation register*
SNR – *signal to noise ratio*
SWR – *sine wave crossing*
TDC – *time to digital converter*
TEM – *time encoding machine*
VCC – *power supply voltage*
XNOR – *exclusive neither disjunction*

NOMENCLATURE

\mathbf{a} – vector
 \mathbf{a}^T – transposed vector
 b – ASDM/AA-ASDM trigger parameter
 C, c – maximum value of the modulus of a signal
 $c(t), \tilde{o}(t)$ – signal time-varying envelope function
 \mathbf{D} – diagonal matrix
 E – energy of the signal
 $e(t)$ – error signal
 F_{\max} – maximum frequency
 \mathbf{G} – matrix
 \mathbf{G}^{-1} – inverse matrix
 \mathbf{G}^+ – pseudo-inverse matrix
 $g(t)$ – signal reconstruction base function
 $\hat{g}(t)$ – periodic approximation of $g(t)$
 $h(t)$ – signal reconstruction base function / impulse response of a filter
 N_{ASDM} – number of switching time instants
 P – signal power
 T – period / Nyquist step
 t – continuous time
 t_n, τ_n – discrete time
 t_k – ASDM/AA-ASDM trigger switching time instants
 $w(t)$ – window function
 $x(t)$ – analog signal
 $\bar{x}(t)$ – mean value
 $\hat{x}(t)$ – reconstructed signal
 $\hat{x}_{L,M,K}(t)$ – reconstructed signal from intervals
 $y(t)$ – output of the integrator
 $z(t)$ – ASDM/AA-ASDM output trigger signal
 α, β – constant
 δ – ASDM/AA-ASDM trigger parameter
 Θ – length of a signal
 $\theta(t)$ – function, which describes the rising and falling edge of the window function
 κ – ASDM/AA-ASDM integrator parameter
 ξ – constant
 $\varsigma(t)$ – integral signal representation
 τ_{\max} – maximum distance between two consecutive trigger switching time instants
 τ_{\min} – minimum distance between two consecutive trigger switching time instants
 Ω – cut-off cyclic frequency
 ω – cyclic frequency

GENERAL DESCRIPTION OF THE WORK

The Urgency of Subject Matter

Everything we encounter in our daily lives - sound, light, temperature, pressure, smell, flavor, etc. are in analog form. On the other hand, nowadays, almost all information is stored and processed in digital form. In order to fill this gap between the real world and the digital world, various analog to digital converters (ADCs) are used.

One very rapidly growing sector, which demands good quality ADCs is neuroscience. In fact, brain neuronal activity generates electrical currents, which in turn generate electrical field potentials which can be measured by using special electrodes, located on the scalp in certain places. [1] The measured signals, called electroencephalogram (EEG) signals, are in analog form and must be digitized (by ADC) to enable easier and much faster signal storage, analysis, processing and research. Since EEG signals contain information about the brain neuronal functions and neurophysiological properties, nowadays, by using advanced signal processing techniques [2], it is possible to understand different processes in human body. Even further, by using advanced signal processing techniques in modern Brain Computer Interface (BCI) systems, it is possible to control "by thoughts", for example, wheelchair, robotic prosthesis, computer, or even a car [3], [4], [5], therefore it is reasonable to believe that BCI is a future technology and it is very important to develop such a field.

In general, BCI is a communication pathway between the brain and an external device. Typical BCI system consists of four main parts: electrodes, differential amplifiers, ADC(s) and data processing / visualization device (i.e. PC). But, nowadays, in order to make it more accessible and convenient to use, a modern BCI systems also include wireless data transmission and a battery as a power source. Despite the fact that development of such systems very increasingly becomes the subject of research, still there exist various problems, weaknesses and limitations.

In order to prolong the life of battery and thus operation time of wireless BCI system, management of energy consumption is a crucial factor. As mentioned before, one very important part of BCI system is ADC, where energy consumption can be significantly reduced. Even further, by using appropriate ADC it is also possible to reduce the amount of information to be transmitted, thus greatly reducing the energy consumption of a transmitter as well. But, excluding low energy consumption, ADC must also ensure proper sampling rate and resolution for good signal quality as well as small physical size on-head device implementations.

Two types of ADCs can be differentiated: synchronous and asynchronous, where each type has its own advantages and disadvantages depending on the end-use application.

For BCI application, it is shown that asynchronous designs, instead of synchronous (which are used in almost all available BCI systems), in ADCs, exhibit better properties such as lower energy consumption, immunity to metastable behavior, modular design, low complicity, exclusion of electromagnetic interference (EMI) and absence of clock jitter [6], [7].

Since EEG signals can be classified as wide dynamic range signals, non-uniform sampling method called Asynchronous Sigma-Delta Modulator (ASDM) has a great potential to improve energy efficiency in BCI system [8], while maintaining other quality requirements. ASDM is a Time Encoding Machine (TEM) which transforms the amplitude information of the signal into time information or time codes without the quantization error that exists in the clocked converters. The method replaces high precision analog amplitude quantizer with 1bit comparator. This reduces the analog circuit complexity. The number of transitions can be controlled by adjusting

step size that is hysteresis of the comparator. This in turn reduces the switching activity and the dynamic power consumption. [9] Latest implementations show that it is possible to create standard ASDM with power consumption not exceeding 7.5 nW [10].

However, due to wide dynamic range that EEG signals have, a high switching activity of ASDM circuit appears when the input signal amplitude is low, causing increased power consumption of a wireless BCI system. The switching activity can be reduced by using the author's proposed Amplitude Adaptive Asynchronous Sigma-Delta modulator.

The Objective of the Work

The main aim of this thesis is to develop an improved method for signal encoding based on ASDM, which allows to reduce the power consumption of the wireless BCI system, while maintaining the desired signal quality. In order to reach the aim, following tasks have been defined:

- to carry out literature review and analysis on EEG signals, including neural activities, action potentials, brain rhythms, EEG signal properties and measurement techniques;
- based on EEG signal and BCI system properties, to define requirements for ADCs;
- based on defined requirements, to carry out literature review and analysis on synchronous and asynchronous ADCs and select the most appropriate ADC;
- to carry out an in-depth analysis and research on ASDM, and identify the points of improvement;
- to carry out an in-depth research on these improvements;
- to develop, test and assess the proposed methods.

The Methodology of Research

In order to complete the tasks of the thesis work, the following methodology was used. Analytic research methods were used for literature review and development of mathematical models. Mathematical calculations and numerical simulations were extensively used to test and assess both the reference design (ASDM) as well as the proposed method (AA-ASDM). This included signal encoding, fast and real-time decoding, error analysis, etc. Experimental measurements and testing were done to validate the proposed method and its performance when connected as a part of BCI system in laboratory environment.

Scientific Novelty and Main Results

The scientific novelty of the thesis is associated with the developed theory and methods for amplitude adaptive ASDM sampling and reconstruction. The main results are:

- a new Amplitude Adaptive Asynchronous Sigma-Delta modulator (AA-ASDM) method for signal-dependent sampling is proposed and described in detail (signal encoding, decoding, fast and real-time decoding principles). The proposed method allows to reduce the switching activity of the circuit by up to 68.85 %, when used for EEG signals;
- an analysis on the AA-ASDM parameters and their impact on the circuit's switching activity, power consumption, speed, precision and complexity;
- two AA-ASDM encoding methods (with additional envelope encoding and without additional envelope encoding) are developed and verified by numerical simulations as well as by circuit simulations;

- several signal reconstruction methods (decoding, fast decoding and real time decoding) from AA-ASDM encoded signals are developed and verified by numerical simulations on different EEG signals;
- a printed circuit board for AA-ASDM is designed, developed and tested;
- a hardware for AA-ASDM based EEG data acquisition system is designed, developed and tested.

Thesis Statements to Be Defended

In this work, the following thesis statements have been promoted and proven:

1. In comparison to ASDM, the decrease of the number of switchings per second of the Amplitude Adaptive Asynchronous Sigma-Delta modulator (AA-ASDM) output trigger is determined by the mean value and the maximum value of the modulus of the signal and the mean value of its estimated envelope function.
2. For electroencephalogram (EEG) signals, the AA-ASDM with the proposed envelope function has up to 68.85 % less average switchings per second of the output trigger, compared to ASDM, while maintaining a 22-bit resolution of AA-ASDM conversion.
3. In comparison to ASDM, by using AA-ASDM it is possible to reduce energy consumption of an event-driven data transmitter by 50 % depending on the circuit parameters.

Practical Value and Approbation

The theory and methods developed within this thesis can be used for signal-dependent sampling and processing with the aim to reduce the power consumption of data acquisition devices, which is of particular importance in wireless sensor networks. The proposed methods are particularly advantageous for wide dynamic range signals, such as EEG, EMG, ECG, EOG, seismic, etc. signals.

The scientific research results of this work have been published in the following papers:

- Ozols K., Shavelis R., *Amplitude Adaptive ASDM without Envelope Encoding*, 2016 24th European Signal Processing Conference (EUSIPCO), Budapest, 2016, pp. 165-169.
- Ozols K., *Implementation of reception and real-time decoding of ASDM encoded and wirelessly transmitted signals*, 2015 25th International Conference Radioelektronika (RADIOELEKTRONIKA), Pardubice, 2015, pp. 236-239.
- Ozols K., Greitans M., Shavelis R., *Amplitude Adaptive Asynchronous Sigma-Delta Modulator*, 2013 8th International Symposium on Image and Signal Processing and Analysis (ISPA 2013), Trieste, 2013, pp. 460-464
- Ozols K., Greitans M., Shavelis R., *EEG Data Acquisition System Based on Asynchronous Sigma-Delta Modulator*, 2012 13th Biennial Baltic Electronics Conference, Tallinn, 2012, pp. 183-186.

The research results of this work have been promoted in the following international conferences:

- "13th Biennial Baltic Electronics Conference", 3-5 October 2012, Tallin, Estonia;

- "8th International Symposium on Image and Signal Processing and Analysis (ISPA 2013)", 4-6 September 2014, Trieste, Italy;
- "The Microwave and Radio Electronics Week 2015 (MAREW2015)", 21-23 April, Pardubice, Czech Republic;
- "24th European Signal Processing Conference (EUSIPCO)", 28 August - 2 September 2016, Budapest, Hungary.

The work has been implemented in the Institute of Electronics and Computer Science, Riga, Latvia, and the results have been applied in the following projects:

- National Research Programme „Cyber-physical systems, ontologies and biophotonics for safe&smart city and society” (SOPHIS) project No. 4 “Development of technologies for secure and reliable smart-city” (GUDPILS);
- European Social Fund’s (ESF) project “R&D Center for Smart Sensors and Networked Embedded Systems” (VieSenTIS) No. ”2009/0219/1DP/1.1.1.2.0/09/APIA/VIAA/020”.

Structure of the Thesis

The volume of the Thesis is 174 pages, and it has following structure. In Section 1, a literature review on neural activities, action potentials, brain rhythms, EEG signal properties and measurement techniques is carried out. Also, in this section, an in-depth analysis of synchronous and asynchronous analog-to-digital converters is performed, in order to identify their advantages and disadvantages as well as suitability for BCI applications. Based on this analysis, one the most suitable ADC for BCI is selected for in-depth analysis in Section 2. This section is dedicated to research on ASDM, particularly on signal encoding and decoding fundamental principles. Also, the main advantages and disadvantages are identified and analyzed. Knowing the main drawbacks of ASDM, in Section 3 the proposed new method, called AA-ASDM is presented. This section describes the main theoretical principles of AA-ASDM signal encoding and reconstruction, as well as fast and real-time reconstruction. In order to verify and assess this theory in practice, in Section 4 various simulations, modeling and physical implementations are carried out for both ASDM (as a reference design) and AA-ASDM. Finally, at the end of this work, in Section 5, conclusions are given. In appendices several mathematical derivations and *Matlab* codes related to ASDM and AA-ASDM are given.

This Doctoral thesis is based on the papers **[11]**, **[12]**, **[13]** **[14]**. Here and further in the text, the references with authors own contribution are highlighted in bold un underlined.

1. BACKGROUND AND RELATED WORK

The main purpose of this section is to describe previous research in the field of analog-to-digital converts (ADC) and choose one the most appropriate for electroencephalogram (EEG) encoding and brain-computer interface (BCI) application as whole. In order to achieve this aim, first of all it is necessary to understand the nature of EEG signals and how BCI systems work. Based on that, the most suitable for EEG signal encoding, synchronous and asynchronous ADC's will be chosen and analyzed against criteria set out in the Section 1.2. After the analysis, the most appropriate/promising ADC for brain-computer interface (BCI) application will be selected for further in-depth analysis in Section 2.

1.1 Electroencephalogram Signals

Human brain has more than 100 billion neurons which conduct electrical impulses and are the core components of the nervous system. These electrical activities can be measured by non-invasive methods from scalp by using electrodes, and the measured signals are called EEG signals. Since human's brains primarily operates in five brain rhythms: delta (0.2-3.9 Hz), theta (4-7.9 Hz), alpha (8-12.9 Hz), beta (13-40 Hz) and gamma (40+ Hz), all these components together are forming the EEG signal. Typically the amplitude of the measured EEG signal from scalp is between 0.5 and 200 μ V.

By using EEG signals, it is possible to create BCI, which can be used to control other electrical or electro-mechanical devices by "thoughts". If simplified, usually modern BCI consists of an electrode (as a sensor), an amplifier, an ADC, a transmitter, a receiver and a computer.

Since a recent trend is to develop wireless BCI devices, management of energy consumption becomes a crucial factor. One very important part of all BCI systems is ADC, where power consumption can be significantly reduced. In addition, by choosing appropriate ADC, it is also possible to reduce the power consumption of the transmitter, by reducing the amount of data to be transmitted.

1.2 Analogue-to-Digital Converters

In order to select the most suitable ADC for BCI, ten different synchronous and asynchronous ADCs are described and analyzed against requirements/criteria, which were set out based on the EEG signal properties and the current situation in the field of the BCI systems. These four main criteria are: Energy Efficiency (the less consumption, the better), Encoding Complexity (the smaller area of silicon die occupied, the better), Resolution (at least 12-bits) and Sampling Rate (at least 400 S/s).

Synchronous Analogue-to-Digital Conversion

Currently, the most popular architectures of analogue-to-digital converters (ADCs) are Flash ADC, Pipeline ADC, Digital Ramp ADC, Tracking ADC, SAR ADC and Sigma-Delta ADC. Since all of these ADCs are driven by a global clock, where ADC states are changed only on rising or falling edges of the clock pulses, such ADCs are called synchronous ADCs. In this section, an overview of mentioned ADCs as well as analysis in relation to requirements is given.

Flash ADC is not suitable for EEG signal encoding, since it does not meet the required resolution (12-bits). Also, the power consumption ($98\,000\ \mu\text{W}$) as well as complexity of the circuit ($0.253\ \text{mm}^2$) is high. In some special cases, the resolution can be increased, but then, the power consumption will be even higher. The complexity and power consumption can be slightly reduced by using two-step Flash ADC, but then there is an increase in latency. Flash ADC is designed for low resolution and high sampling rate applications, and for BCI applications there is no need for GS/s sampling rate, since the maximum EEG signal frequency is 200 Hz; [15]

Pipeline ADC meets the requirements of resolution and sampling rate, but the power consumption is high ($30\,000\ \mu\text{W}$) and the complexity of the circuit is very high ($0.860\ \text{mm}^2$). Pipeline ADC could be used for EEG signal encoding, but it is clear that it is not the best option for BCI, where energy efficiency and small size play crucial role; [16]

Digital Ramp ADC can be implemented in a very small dimensions on the silicon die ($0.017\ \text{mm}^2$), which makes it very attractive for BCI applications. On the other hand, although it can ensure the necessary resolution and sampling rate, the power consumption of the circuit is high ($3800\ \mu\text{W}$), which makes it less attractive for BCI applications; [17]

Tracking ADC is able to ensure the necessary resolution and sampling rate, but the power consumption ($50\,000\ \mu\text{W}$) and complexity of the circuit ($0.350\ \text{mm}^2$) is too high for BCI; [18]

SAR ADC is one of the best choices for EEG signal encoding and BCI as whole, since it can ensure not only the necessary resolution and sampling rate, but also very low power consumption ($0.100\ \mu\text{W}$), despite the fact that complexity of the circuit is relatively high ($0.300\ \text{mm}^2$); [19]

Sigma Delta ADC as SAR ADC is very attractive for EEG signal encoding and BCI application as whole. It offers high resolution (up to 32-bits) and low power consumption ($13.3\ \mu\text{W}$ for 12-bits) and proper sampling rate. The only disadvantage is the complexity of the circuit, which occupies more space on silicon die ($0.510\ \text{mm}^2$). [20]

Asynchronous Analogue-to-Digital Conversion

Although some of synchronous ADC architectures fit the defined requirements and could be used for EEG and BCI applications, most of them exhibit poor properties in terms of electromagnetic interference (EMI), complexity of circuit, sensitivity against power supply voltage, temperature and development process parameter variations, delays, etc. [6], [7].

An alternative to synchronous ADCs is asynchronous ADCs, which due to its great properties often are used for encoding of non-stationary signals. [21], [8] Since EEG signals are wide dynamic range signals, non-uniform sampling methods have a great potential to improve energy efficiency, reduce complexity of the encoding and avoid unnecessary EMI in BCI [8]. Therefore, in this section, an overview of the most popular non-uniform sampling methods as well as analysis in relation to set out requirements are given.

Zero ADC can't be used for EEG signal encoding, since it can't meet the required resolution, even though it has very simple architecture and potentially low power consumption; [22]

Sinewave ADC could be used for EEG signal encoding, due to its low complexity circuit and potentially low power consumption, but at the time of writing this thesis, no physical implementations could be found, therefore it was not possible to estimate its performance; [23]

Level Crossing ADC can be used for EEG signal encoding, since it offers simple circuit and low power consumption (from $582\ \text{nW}$). But this is valid only for low resolution applications. For desired 12-bits, both the complexity of the circuit ($0.300\ \text{mm}^2$) as well as power consumption ($9\ \mu\text{W}$) increase and make it less attractive for BCI applications; [24]

ASDM exhibit excellent properties for EEG signal encoding and BCI application as whole. It offers very low power consumption (from 9.4 nW) and complexity of the circuit (0.026 mm²), while preserving necessary resolution and sampling rate. The only ASDM disadvantage is more complex and resource demanding signal reconstruction; [25]

Peak Sampling ADC, basically, is an energy efficient modification of SAR ADC and potentially could be used for EEG signal encoding. But, since at the time of writing this thesis, there was only one physical implementation (with 8-bits), it was not possible to estimate its true performance. [26]

1.3 Conclusions

There are trade-offs for each of the listed ADCs. A comparison is given in the Table 1.1.

Table 1.1: Comparison of different types of ADCs, where in each type the most suitable ADC for EEG/BCI application is selected, based on the set out criteria

ADC type	Power Consumption (μ W)	Core Area (mm ²)	Resolution (bits)	Max. Sampling Rate (MS/s)
Flash ADC	90 800	0.253	8	2 000
Pipeline ADC	30 000	0.860	12	25
Digital Ramp ADC	3 800	0.017	12	0.746
Tracking ADC	50 000	0.350	12	0.0005
Successive Approx. ADC	0.100	0.300	12	0.020
Sigma-Delta ADC	13.30	0.510	12	0.0005
Sinewave Crossing ADC	110*	-	12*	60*
Level Crossing ADC	1700	0.300	12	0,228
ASDM	0.0094	0.026	12	0.0005
Peak Sampling ADC	15	0.230	8	1.25

By taking into account analysis in Section 1.2, and overview in Table 1.1, SAR ADC and ASDM exhibit the most suitable properties for EEG signal Encoding and BCI application as whole. In this case, by considering parameters of both ADCs in Table 1.1 and advantages of asynchronous over synchronous designs, such as [6], [7]: lower energy consumption, electromagnetic emissions, sensitivity against power supply voltage, temperature and development process parameter variations, delays and complexity; better modularity and interlinking between individual circuit units; higher potential for energy efficiency improvement, if used for EEG signals; and absence of overheads and problems associated with distributing clock signals; an ASDM method is chosen for further in-depth analysis, research and improvements.

Although ASDM has many advantages, the use of asynchronous systems in real life applications are limited due to incompatibility with classical (synchronous) systems, which results in fewer research studies in this area, thus slowing down its development. Therefore, the author of this work believes that it is very important to understand the true potential of asynchronous systems and will dedicate himself to carry out the research in the field of ASDM.

2. ASYNCHRONOUS SIGMA-DELTA MODULATOR

2.1 Signal Encoding

ASDM is a clock-less ADC, which converts amplitude information of the input signal $x(t)$ into time information or time sequence t_k in a very energy efficient way. The block diagram of the ASDM is shown in Figure 2.1. It consists of an integrator with parameter κ , a non-inverting Schmitt trigger with parameters δ and b and a negative feedback. The values of these parameters determine the average switching rate of the trigger. [27] [28]

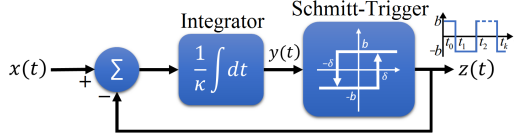


Figure 2.1: Asynchronous sigma-delta modulator (ASDM) block diagram. [27] [11]

The input signal $x(t)$ of ASDM is bounded in amplitude as $|x(t)| \leq c < b$ [28]. Since trigger output $z(t)$ has either b or $-b$ value, the integrator input is either $x(t) + b$ or $x(t) - b$. It follows the integrator output $y(t)$ is strictly increasing or decreasing function for $t \in [t_k, t_{k+1}]$, and $y(t_k) = (-1)^k \delta$. The relationship between the binary output $z(t)$ and the input signal $x(t)$ of the ASDM for $t_{k+1} > t_k$, and integers $k \in \mathbb{Z}$, is given by the integral equation [29]

$$\int_{t_k}^{t_{k+1}} x(t) dt = (-1)^k [2\kappa\delta - b(t_{k+1} - t_k)] \quad (2.1)$$

Due to $|x(t)| \leq c < b$ the distances between consecutive triggering points t_k and t_{k+1} are bounded [30]

$$\tau_{min} = \frac{2\kappa\delta}{b+c} \leq t_{k+1} - t_k \leq \frac{2\kappa\delta}{b-c} = \tau_{max} \quad (2.2)$$

Figure 2.2 shows the operation of ASDM on an Electroencephalogram signal.

Assuming that the amplitude of the input signal $A_0 = 1$, the signal to noise ratio of ASDM can be calculated as follows: [31]

$$SNR = 10 \log_{10} \left(\frac{P_s}{P_N} \right) = 10 \log_{10} \left(\frac{3}{8} \frac{\bar{T}}{2T_{res}^2 F_{max}} \right) = 10 \log_{10} \frac{3}{8} \frac{\bar{T}}{2F_{max}} + 20 \log_{10} f_{res}, \quad (2.3)$$

where P_s is the power of a sinusoidal signal, P_N is the total noise power within bandwidth $2F_{max}$, \bar{T} is a constant mean value of duration of two consecutive pulses T_k , but $T_{res} = \frac{1}{f_{res}}$ denotes the resolution of the Time to Digital converter (TDC). By knowing SNR, it is possible to calculate ENOB of an ideal ASDM: $ENOB = \frac{SNR-1,76}{6,02}$. [32]. It follows that by doubling the frequency f_{res} of TDC, SNR and ENOB of ASDM increase by 6 dB and 1 bit, respectively.

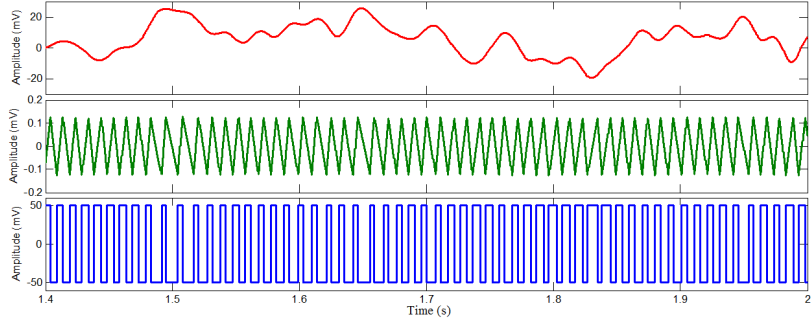


Figure 2.2: Operation of ASDM. EEG signal (red line) and corresponding ASDM integrator output $y(t)$ (green line) and ASDM trigger output $z(t)$ (blue line).

2.2 Signal Recovery

If the ASDM input signal $x(t)$ is represented as

$$x(t) = \sum_{n \in \mathbb{Z}} a_n g(t - \tau_n), \quad (2.4)$$

where $g(t) = \frac{\sin \Omega t}{\pi t} = \frac{\Omega}{\pi} \text{sinc}(\Omega t)$ is the impulse response of an ideal LPF with cutoff frequency Ω , $\tau_n = \frac{t_k + t_{k+1}}{2}$ and a_n are the coefficients to be estimated, then from (2.1) and (2.4) follow that the coefficient values can be expressed as [28]

$$\mathbf{a} = \mathbf{G}^+ \mathbf{q}, \quad (2.5)$$

where \mathbf{G}^+ is the pseudoinverse matrix of \mathbf{G} and elements of vector \mathbf{q} and matrix \mathbf{G} are $q_k = (-1)^k (2k\delta - b(t_{k+1} - t_k))$, $G_{kn} = \int_{t_k}^{t_{k+1}} g(t - \tau_n) dt$. [28]

As graphically shown in Figure 2.3, by finding coefficient values \mathbf{a} (black bars), which are multiplied by sinc functions $g(t - \tau_n)$ and summed together, it is possible to reconstruct the original signal $x(t)$ (red line).

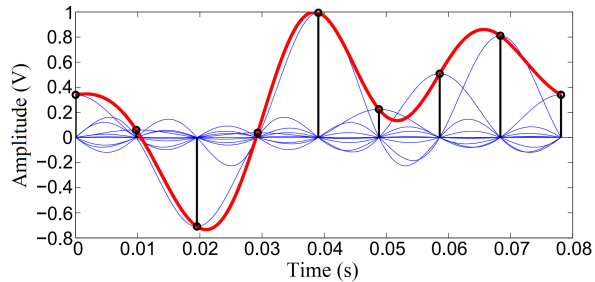


Figure 2.3: Visualization of signal recovery. Coefficients \mathbf{a} (black bars), sinc functions $g(t - \tau_n)$ (blue lines), reconstructed EEG signal (red line).

Unfortunately, since numerical calculation of elements $g_{k,n}$ from matrix \mathbf{G} requires to assign the function $g(t)$ with sufficiently fine step and there is a need to do a matrix \mathbf{G} pseudoinversion, the signal recovery method described above is time and resource consuming and thus can not be used for real-time applications. In order to increase the speed of signal reconstruction, following expression, which describes the reconstructed signal, is used [13], [33]:

$$\hat{x}(t) = \frac{j2\pi F_{\max}}{M} \sum_{m=-M}^M m v_m e^{jm \frac{2\pi F_{\max}}{M} t} \quad (2.6)$$

where unknown coefficients v_m can be found by $\mathbf{v} = \xi \Phi^+ \mathbf{RDP}^{-1} \mathbf{q}$ (the elements of the expression can be found in full doctoral thesis).

However, despite the fact that by using the fast signal recovery method it is possible to reconstruct the original signal significantly faster (see Section 4.1.1), it is not possible to reconstruct the signal in real-time, since prior to reconstruction it is necessary to store time instants from the ASDM output signal. In order to be able to reconstruct the signal in real time, short time interval reconstruction method should be used [34]:

$$\hat{x}(t) = \sum_{m \in Z} \hat{x}_m(t) w_m(t),$$

where $t \in [t_{mJ}, t_{mJ+L}]$, but $w_m(t)$ is a window function, defined as in (2.7). In this case, $m = 0, 1, 2, \dots$ designates the order number of the interval, J determines the number of switchings, after which the reconstruction of the next interval can start, but L is a number of switching instants, which determines the length of the interval (see Fig. 2.4).

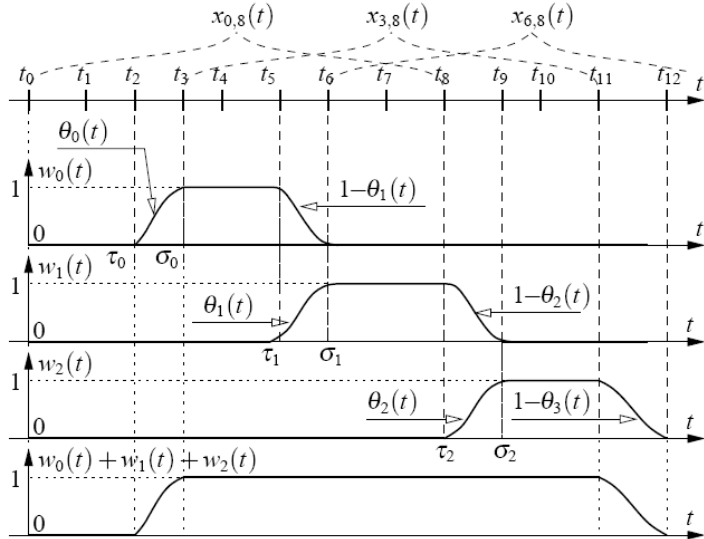


Figure 2.4: Real-time signal reconstruction by using interval approach [34]. In this particular case/figure, $t_0 = 0, L = 8, M = 2, K = 1(J = 3), x_{mJ,L}(t)$.

$$w_m(t) = \begin{cases} 0, & \text{if } t \notin (\tau_m, \sigma_{m+1}], \\ \theta_m(t), & \text{if } t \in (\tau_m, \sigma_m], \\ 1, & \text{if } t \notin (\sigma_m, \tau_{m+1}], \\ 1 - \theta_{m+1}(t), & \text{if } t \in (\tau_{m+1}, \sigma_{m+1}], \end{cases} \quad (2.7)$$

where $\tau_m = t_{mJ+M}$, $\sigma_m = t_{mJ+M+K}$ and $\theta_m(t) = \sin^2 \frac{\pi(t-\tau_m)}{2(\sigma_m-\tau_m)}$.

2.3 Advantages and Disadvantages

The main benefits of ASDM are low energy consumption, immunity to metastable behavior, modular design, significant exclusion of electromagnetic interference (EMI), the absence of clock, low complicity, continuous-time signal processing, etc, which makes it suitable for BCI applications. [35], [36], [37]

Despite the fact that ASDM has a long list of advantages, which makes it one of the best choices for EEG encoding and BCI application, it still has some disadvantages. The main inefficiency is related to over-triggering, which occurs when ASDM is applied to wide dynamic range signals such as EEG signals (see Fig. 2.5). [12] Due to wide dynamic range that these

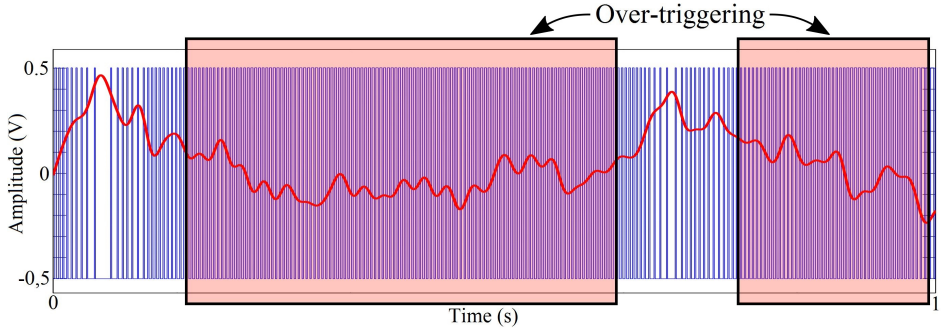


Figure 2.5: EEG signal (red line) and ASDM trigger output signal (blue line).

signals have, an unnecessary high switching activity of ASDM circuit appears when the input signal amplitude is low, causing increased power consumption of a wireless BCI system.

2.4 Conclusions

The main ASDM inefficiency is related to over-triggering, which occurs when ASDM is applied to wide dynamic range signals. This is because the ASDM circuit parameters are chosen considering the maximum value that is never exceeded by the signal. Since the envelope of the signal changes over time, the proposition is: instead of constant value to consider the time-varying maximum value, which is also never exceeded by the signal. This could allow to reduce the over-triggering of the circuit and thus the power consumption of whole wireless BCI system, since less switchings instants (events) will be necessary to be transmitted, which greatly reduces the power consumption of the transmitter. The proposed amplitude adaptive method is described in next Section 3.

3. AMPLITUDE ADAPTIVE ASYNCHRONOUS SIGMA-DELTA MODULATOR

In order to overcome the main ASDM inefficiency, a new method, called Amplitude-Adaptive Asynchronous Sigma-Delta modulator (AA-ASDM) is proposed and described in this Section.

Since envelope of the signal changes over time, the proposition of this work is, instead of constant value b , to consider the time-varying maximum value $c(t)$, which is also never exceeded by the signal, i.e. to change the ASDM circuit parameter b according to $c(t)$ to ensure that maximum distance T between two consecutive trigger switching times t_k and t_{k+1} is [12]:

$$\tau_{\max 2}(t) = \frac{2\kappa\delta_2}{b_2(t) - c(t)} = \text{const.} = T, \quad (3.1)$$

where b_2 and δ_2 are hysteresis parameters of the trigger. In this case, the difference $b_2(t) - c(t)$ must be constant and thus $b_2(t)$ can be written as $b_2(t) = c(t) + \beta C$, where C is the maximum value of $|x(t)|$ and $\beta > 0$. The minimum distance becomes [12]

$$\tau_{\min 2}(t) = \frac{2\kappa\delta_2}{b_2(t) + c(t)} = \frac{T}{1 + 2c(t)/(\beta C)}. \quad (3.2)$$

The block diagram of proposed AA-ASDM, which is an enhanced version of ASDM, is shown in Figure 3.1. [12] In addition to ASDM circuit (see Fig. 2.1), there is an envelope detector with

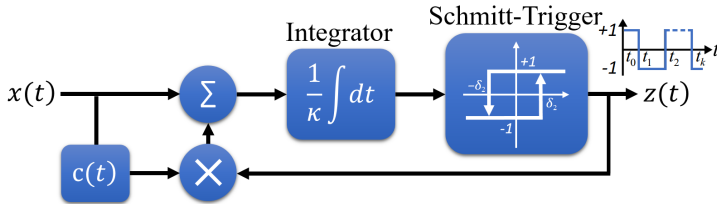


Figure 3.1: Amplitude Adaptive Asynchronous Sigma-Delta modulator block diagram.

output $c(t)$ connected to the feedback loop. Now, instead of the equation (2.1), the relationship between the switching instants t_k of the AA-ASDM output $z(t)$ and the input signal $x(t)$ for $t_{k+1} > t_k$, and integers $k \in \mathbb{Z}$, is given by the following equation:

$$\int_{t_k}^{t_{k+1}} x(t) dt = (-1)^k [2\kappa\delta - \int_{t_k}^{t_{k+1}} c(t) dt], \quad (3.3)$$

where κ and δ are AA-ASDM circuit parameters. The proposed method allows to reduce the over-triggering of the circuit and thus the power consumption of wireless BCI system.

Based on this, two amplitude adaptive methods: 1) AA-ASDM with additional envelope encoding (Section 3.1); and 2) AA-ASDM without additional envelope encoding (Section 3.2); are proposed and described.

3.1 AA-ASDM with additional envelope encoding

In this case, the envelope signal $c(t)$ is also needed for recovery of $x(t)$, therefore it is encoded by another ASDM (see Fig. 3.2). [12] Now, for AA-ASDM1 to be advantageous over ASDM,

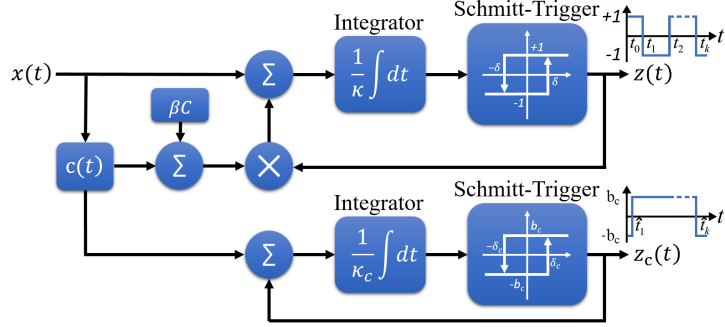


Figure 3.2: Amplitude Adaptive Asynchronous sigma-delta modulator with additional envelope encoding block diagram (AA-ASDM1).

the signal $c(t)$ must have low frequencies in comparison to $x(t)$.

In this case, the complexity of signal recovery increases, but power consumption of the wireless BCI system decreases, due to fewer trigger switchings. The effectiveness of this AA-ASDM1 approach is estimated by simulations in Section 4.1.2. Regardless of the decrease of the number of switchings, the perfect recovery of the original signal from the obtained time sequence is still possible. [12]

In order to recover the encoded signal, the first step is recovery of envelope signal $c(t)$. When $c(t)$ is found, the original signal $x(t)$ is recovered from the given time sequence t_k by finding the unknown coefficients by the following equation [33], [12]:

$$\hat{\mathbf{a}} = \mathbf{G}^+ \mathbf{q}, \quad (3.4)$$

where $q_k = (-1)^k (2\kappa\delta - \beta C(t_{k+1} - t_k) - \int_{t_k}^{t_{k+1}} c(t) dt)$ and $G_{kn} = \int_{t_k}^{t_{k+1}} g(t - \tau_n) dt$.

Similar to ASDM (see Section 2.2), by using this signal recovery method, the reconstruction is time and resource consuming therefore fast and real-time signal reconstruction methods are considered. Both methods and their derivations of expressions can be found in the full thesis work.

Although AA-ASDM1 is advantageous over ASDM in terms of switching activity, the efficiency of this method can be improved, if the time-varying envelope of the signal is not additionally encoded and transmitted in order to recover the original signal.

3.2 AA-ASDM without additional envelope encoding

Further studies have led to a solution which not only solves the AA-ASDM1 problem, where the envelope function must be encoded by additional ASDM, but also allows to reduce the switching activity of the ASDM circuit even more. The proposed method shows how to choose the

time-varying envelope in such a way, that there is no need to encode and transmit information about the envelope and to be able to recover the signal from the obtained time sequence.

The relationship between the switching instants t_k of the AA-ASDM2 output $z(t)$ and the input signal $x(t)$ is the same as in AA-ASDM1, only in this case, the proposition is to use the time-varying envelope function as $\tilde{o}(t) = 0.25 + x^2(t)$, where the inequality $\tilde{o}(t) \geq |x(t)|$ holds for all $x(t) \in [-1, 1]$. This function does not require any additional encoding scheme to be able to reconstruct the original signal (see Fig. 3.3). **[14]**

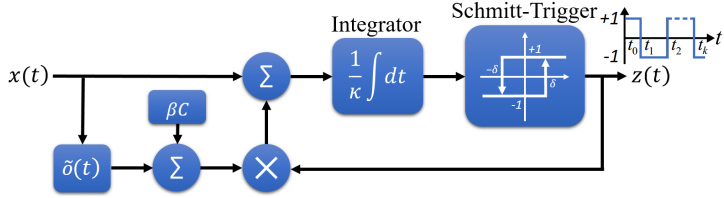


Figure 3.3: Amplitude Adaptive Asynchronous sigma-delta modulator without additional envelop encoding block diagram AA-ASDM2.

The input signal $x(t)$ can be represented as $x(t) = \sum_{n=0}^{N-1} \tilde{d}_n g_n(t)$, where \tilde{d}_n are unknown coefficients and $g_n(t)$ are the chosen base functions. The unknown coefficients $\tilde{\mathbf{d}}$ are found by minimizing the total error value **[14]**:

$$\sum_{k=1}^{K-1} \left(\tilde{\mathbf{d}}^T \cdot \mathbf{g}_k + (-1)^k \tilde{\mathbf{d}}^T \cdot \hat{\mathbf{G}}_k \cdot \tilde{\mathbf{d}} - \tilde{q}_k \right)^2, \quad (3.5)$$

where $\tilde{q}_k = (-1)^k [2\kappa\delta - (\beta C + 0.25)(t_{k+1} - t_k)]$, $\hat{\mathbf{G}}_{k_m n} = \int_{t_k}^{t_{k+1}} g_m(t) g_n(t) dt$, but

$$\mathbf{g}_k = \begin{bmatrix} \int_{t_k}^{t_{k+1}} g_0(t) dt \\ \int_{t_k}^{t_{k+1}} g_1(t) dt \\ \vdots \\ \int_{t_k}^{t_{k+1}} g_{N-1}(t) dt \end{bmatrix}. \quad (3.6)$$

Different base functions $g_n(t)$ can be chosen for representing the input signal $x(t)$. If $g_n(t)$ are chosen to be sinc functions, as in ASDM and AA-ASDM1 case, two problems occur: 1) these functions are not well suited for representing time-limited signals; 2) calculation of \mathbf{g}_k and $\hat{\mathbf{G}}_k$ is both time consuming and not perfectly precise since no analytical solutions of the integrals exist. In order to solve these problems, the proposition of this work is to use Fourier series instead of sinc functions for the original signal representation. **[14]**

By using Fourier series, given the output sequence $\{t_k\}_{k=1,2,\dots,K}$ with the corresponding time period $\Theta = t_K - t_1$, the input signal for $t \in [t_1, t_K]$ is expressed as **[14]**

$$x(t) = \tilde{d}_0 + \sum_{m=1}^M \left(\tilde{d}_m \cos\left(m \frac{2\pi}{\Theta} t\right) + \tilde{d}_{m+M} \sin\left(m \frac{2\pi}{\Theta} t\right) \right), \quad (3.7)$$

where the upper limit M follows from the bandwidth Ω of the signal $M = \left\lfloor \frac{\Omega\Theta}{2\pi} \right\rfloor$. Such a representation of $x(t)$ is both well suited for expressing time-limited signals of length Θ and allows fast and precise calculation of \mathbf{g}_k and $\hat{\mathbf{G}}_k$. The real-time signal reconstruction is carried out by using the same approach as in "AA-ASDM1" case. **[14]**

AA-ASDM2 allows not only to reduce the switching activity of the ASDM circuit even more, compared to AA-ASDM1, but it also decreases the speed and delay of the signal reconstruction meanwhile keeping the desired precision (see Section 4.1.3). **[14]**

The ratio between the minimum value of a number N_{ASDM} of switching time instants and the maximum value of $N_{\text{AA-ASDM}}$ can be obtained from the following expression:

$$\frac{N_{\text{ASDM min}}}{N_{\text{AA-ASDM max}}} = \frac{1 - \gamma_x + \alpha}{\gamma_c + \gamma_x + \alpha}. \quad (3.8)$$

where $\gamma_x = \bar{x}_{abs}/C$ and $\gamma_c = \bar{\delta}/C$ are coefficients and their elements are $\bar{x}_{abs} = \frac{1}{\Theta} \int_0^\Theta |x(t)| dt$, C is a maximum amplitude of absolute value of the input signal $x(t)$, but $\bar{\delta} = \frac{1}{\Theta} \int_0^\Theta \tilde{\delta}(t) dt$ is the mean value of time-varying envelope $\tilde{\delta}(t)$ of the input signal $x(t)$. In AA-ASDM2 case, the maximum ratio is 4.

It follows that AA-ASDM is advantageous over ASDM for signals having high peak-to-peak amplitudes in comparison to their mean absolute values. All derivations of expressions can be found in the full thesis work.

3.3 Conclusions

In order to overcome the main ASDM inefficiency, in this Section, a new method, called AA-ASDM was proposed and described in detail. The proposition was, instead of constant value trigger parameter b , to consider the time-varying maximum value, which is never exceeded by the signal, i.e. to change the ASDM circuit parameter b according to $c(t)$ to ensure that maximum distance T between two consecutive trigger is equal to Nyquist step T . Both presented approaches: AA-ASDM1 and AA-ASDM2 are particularly advantageous over ASDM if used for wide dynamic range signals. Theoretically, it is possible to achieve up to 75 % less trigger switchings if AA-ASDM instead of ASDM is used. In order to verify and assess the theory, AA-ASDM must be simulated, modeled and implemented as physical device. This is done in the next Section 4.

4. EXPERIMENTAL RESEARCH

In order to verify and assess the theory, developed in Section 3, in practice, in this Section various simulations (in *Matlab*), modeling (in *SIMatrix*), design (in *Altium Designer*) and physical implementations of ASDM (as a reference design) and AA-ASDM are carried out.

4.1 Simulations

In this section, both ASDM and AA-ASDM approaches are tested on real electroencephalogram (EEG) signals acquired by the 14-channel *Emotiv EPOC* headset. Considering typical EEG signal frequencies (see Section 1.1), all signals are low-pass filtered up to 49Hz in order to remove the noise prior to encoding.

4.1.1 Asynchronous Sigma-Delta Modulator

The experimental simulation results of ASDM encoding, decoding and fast and real-time decoding as well as estimation of speed, error, resolution, etc. are shown in the full thesis and partially in Table 4.1 and Table 4.2 (see next Sections).

4.1.2 AA-ASDM with additional envelope encoding

Based on the theory, described in Section 3.1, AA-ASDM1 is simulated and assessed in this Section. First, the parameters of the AA-ASDM1 must be set in such a way that maximum distance between two consecutive trigger switchings $t_{k+1} - t_k$ does not exceed the Nyquist step, i.e. $\tau_{\max} \leq \frac{1}{2F_{\max}}$. In this case, AA-ASDM1 parameters are set as follows: $\kappa = 1$, $b_2 = c(t) + \beta C$, where β is a constant (0.1, 0.3, 0.7, 1, 1.3, 1.9 or 2.5) and C is a maximum amplitude of absolute value of the EEG signal, but δ_2 is calculated from the equation $\delta_2 = 0.9\beta CT/2$. For envelope encoding, the parameters are set as $\kappa_c = 1$, $b_c = 2C$ and $\delta_c = C/4F_{\max_c}$.

The example of the input EEG signal and its estimated envelope function, when $\beta = 0.1$, is shown in Fig. 4.1. If more precise (more rapid) envelope (dashed line in Fig. 4.1) is used, then

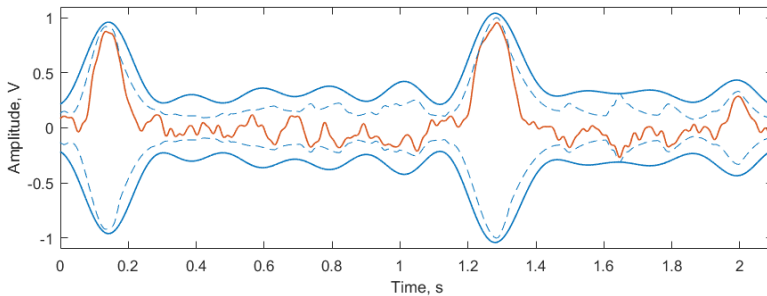


Figure 4.1: Input EEG signal (red line) and its low frequency envelope functions (blue lines).

less triggering occurs at the output of the upper trigger (see Fig. 3.2), however, more switchings are required to encode the envelope.

The simulation results for different β values and EEG signals show that in average there are $396+10=406$ (upper+lower trigger) switchings when $\alpha = \beta = 0.1$, 220 (when $\alpha = \beta = 0.3$), 166 (0.7), 153 (1), 146 (1.3), 139 (1.9), 135 (2.5).

If compared to ASDM, in Fig. 4.2 it can be seen that AA-ASDM1 maximum distances (close to T) occur all the time and the values $\hat{t}_{k+1} - \hat{t}_k$ are more spread, which allows to reduce the number of switching time instants.

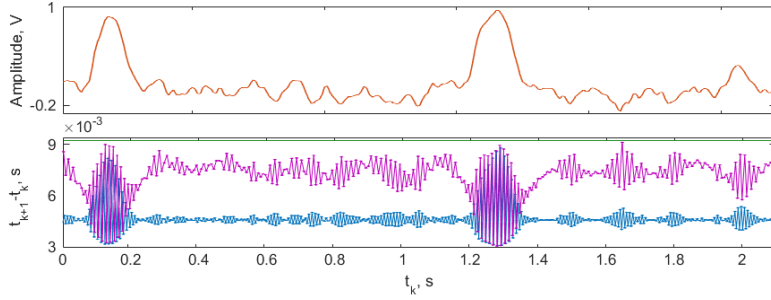


Figure 4.2: EEG signal (red line) and the obtained distances between consecutive trigger switchings for ASDM (blue line) and AA-ASDM1 (pink line), and Nyquist step (green line).

AA-ASDM1 encoded signal can be recovered by using two approaches: *Classical reconstruction* and *Fast reconstruction*. As experimental simulation results show, the *Fast reconstruction* method is up to 228 times faster than *Classical reconstruction*. In order to reconstruct in real time, the reconstruction is carried out in short time intervals as described in Section 2.2.

Simulation results show that the average SNR for both *Classical reconstruction* and *Fast reconstruction* approaches lies within the range of ≈ 131 -132dB (≈ 22 bits), but for real time reconstruction ≈ 123 dB (≈ 20 bits).

4.1.3 AA-ASDM without additional envelope encoding

AA-ASDM2 parameters are set as in previous Section 4.1.2. In this case, the envelop function is set as $c(t) = 0.25 + x^2(t)$.

The example of the input signal and its estimated envelope ($\alpha = 0.1$), is shown in Fig. 4.3.

The distances between consecutive trigger switching time instants, when $\alpha = \beta = 1$, are shown in Fig. 4.4. Comparing Fig. 4.1 (AA-ASDM1) and Fig. 4.3 (AA-ASDM2), it can be seen that in AA-ASDM2 case the envelope is more precise and thus the number of trigger switching time instants is lower, as it can be also seen in Table 4.1.

Table 4.1: Comparison number of trigger switching time instants per second and corresponding energy saving of the transmitter for ASDM, AA-ASDM1 and AA-ASDM2

As the $\alpha = \beta$ values grow, the advantage (in switching activity) of AA-ASDM2 over ASDM becomes less, however, it is not recommended to choose too high these values since the variance of distances between consecutive trigger times reduces and more precision (more bits) is needed to measure the distances. Too low $\alpha = \beta$ values are not recommended as well since high switching activity appears in both cases.

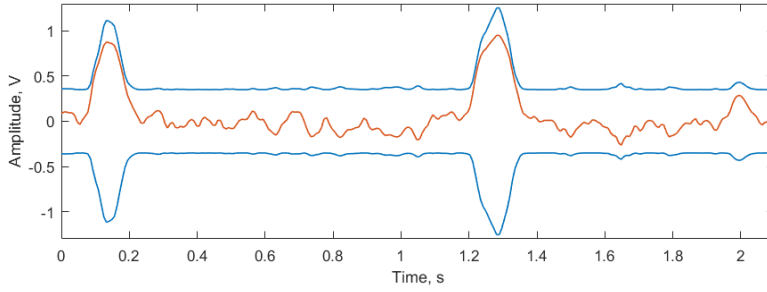


Figure 4.3: Input EEG signal (red line) and its envelope function (blue line).

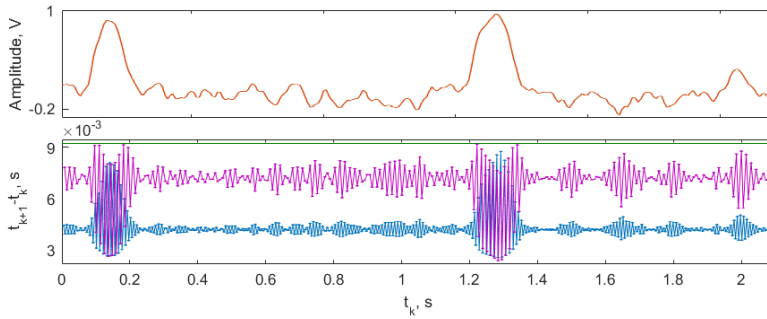


Figure 4.4: EEG signal (red line) and the obtained distances between consecutive trigger switching time instants for ASDM (blue line) and AA-ASDM (pink line), and Nyquist step (green line).

$\alpha = \beta$:	0.1	0.3	0.7	1	1.3	1.9	2.5
N_{ASDM} :	1184	468	263	217	192	166	152
$N_{AA-ASDM1}$:	406	220	166	153	146	139	135
AA-ASDM1 Energy saving:	65.69 %	52.90 %	37.11 %	29.55 %	24.01 %	16.42 %	11.48 %
$N_{AA-ASDM2}$:	369	200	150	139	132	126	122
AA-ASDM2 Energy saving:	68.85 %	57.20 %	42.91 %	36.00 %	31.18 %	24.38	19.96 %

For AA-ASDM2, the experimental simulation results show, that it takes in average 0.09s to reconstruct one original signal fragment with a length of 0.5s, when $\alpha = \beta = 1$ (see Table 4.2). As can be seen in Table 4.2, the reconstruction speed vary depending on the length of the fragment needed to be reconstructed. Also, it can be seen, that the signal reconstruction for AA-ASDM is more time consuming than for ASDM. This is due to fact that the optimization algorithm, which minimizes the expression (3.5), is used to find the unknown coefficients needed for signal reconstruction. Besides that, it can be seen that by using AA-ASDM it is possible to achieve practically the same precision of the reconstructed signal as in the ASDM case. It can be concluded that the performance of AA-ASDM is admissible, since it fulfills the requirements

set out in Section 1.2. Experimental simulations shows that the use of real-time reconstruction algorithm do not affect the average SNR value.

Since all AA-ASDM2 performance indicators are better than AA-ASDM1, except the reconstruction speed, for further experimental research AA-ASDM2 is used.

Table 4.2: Comparison of ASDM and AA-ASDM2 reconstruction speed for different $\alpha = \beta$ values and signal lengths

ASDM									
	0.1 second long input signal			0.5 second long input signal			1 second long input signal		
$\alpha = \beta$	Time (s)	N_{ASDM}	SNR (dB)	Time (s)	N_{ASDM}	SNR (dB)	Time (s)	N_{ASDM}	SNR (dB)
0.1	0,0015	63	124	0,0073	458	123	0,0249	1184	124
1	0,0040	19	135	0,0058	95	136	0,0170	217	136
2.5	0,0161	14	137	0,0055	69	137	0,0088	152	139

AA-ASDM2									
	0.1 second long input signal			0.5 second long input signal			1 second long input signal		
$\alpha = \beta$	Time (s)	$N_{AA-ASDM}$	SNR (dB)	Time (s)	$N_{AA-ASDM}$	SNR (dB)	Time (s)	$N_{AA-ASDM}$	SNR (dB)
0.1	0,0060	31	128	0,1800	139	127	0,6231	369	129
1	0,0063	15	133	0,0900	67	135	0,4457	139	137
2.5	0,0093	13	138	0,3006	58	137	0,7603	122	138

4.2 Modeling

In order to develop a working AA-ASDM2 hardware prototype and estimate its properties, first an electric circuit model with existing electronic components must be developed, simulated and analyzed for both ASDM and AA-ASDM2. To reach this aim, *SIMatrix* circuit simulation software is used for transient analysis and power consumption estimation of ASDM, AA-ASDM2 and On-Off-Keying (OOK) transmitter circuits.

4.2.1 Asynchronous Sigma-Delta Modulator

Electric circuits of the ASDM and corresponding OOK transmitter as well as experimental modeling results are shown in the full thesis.

4.2.2 AA-ASDM without additional envelope encoding

The electrical circuit of the AA-ASDM2 is similar to the ASDM circuit, only in this case it is supplemented by an Analog Multiplier (*MLT04*) and a Voltage Follower (*OpAmp1*) (see Fig. 4.5), where by changing the value of capacitor $C1$, it is possible to adjust the distance between two consecutive trigger switching time instants. In order to make a comparison between ASDM and AA-ASDM2 circuits, the parameters in both circuits are set to be equal.

Simulation results of the AA-ASDM2 circuit are shown in Fig. 4.6. The experimental modeling shows that the average power consumption of the AA-ASDM2 circuit is $\approx 60\%$ higher (≈ 231 mW), compared to ASDM (≈ 145 mW). But, it should be noted that simulations were

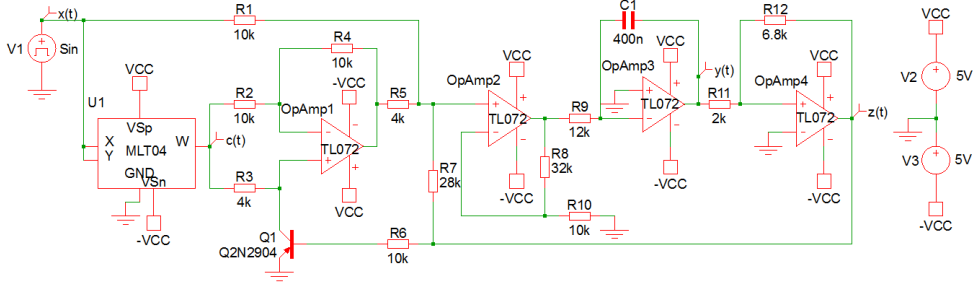


Figure 4.5: AA-ASDM2 electrical scheme.

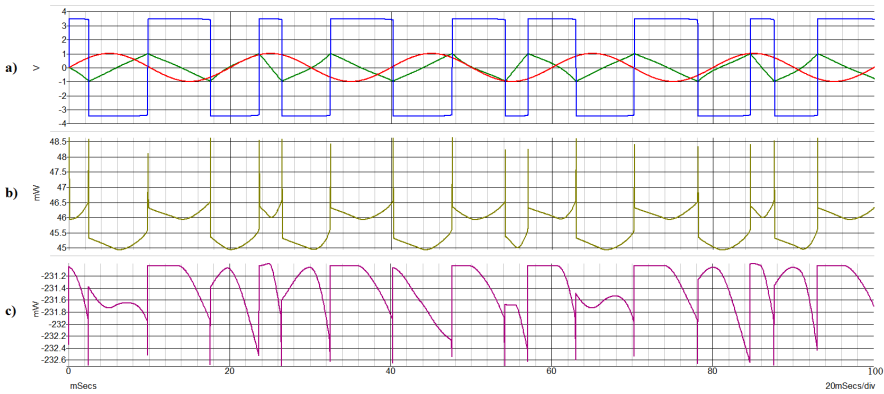


Figure 4.6: Operation of AA-ASDM2. a) Input signal (red line), integrator output (green line) and trigger output (blue line); b) Power consumption of the trigger; c) power consumption of the whole circuit.

made only to verify the working principles of both circuits and the power consumption values are just indicative, as it is possible to develop an ASDM circuit with 7.5nW power consumption as shown in [10]. This means, if the AA-ASDM2 circuit is implemented in the same technology as shown in [10], the increase of power consumption by 60 % compared to ASDM would give an overall power consumption of the AA-ASDM circuit: 12nW.

As mentioned before, the main power consumer of a BCI system is a transmitter, therefore, it is more important to reduce the amount of information to be transmitted. Therefore, an event-driven transmitter is also modeled and simulated together with AA-ASDM2.

For this particular BCI application, due to its great properties, an OOK technique is used for wireless data transmission. It has several advantages - simple architecture, good performance in the presence of co-channel interference, robust when exposed to vibration and shock, and major criteria - small dimensions for on-head device implementation. [11] Simple OOK implementation for AA-ASDM2 output transmission, where a short pulses filled with carrier frequency are generated each time the AA-ASDM2 output is changing its state to opposite, is shown in Fig.

4.7.

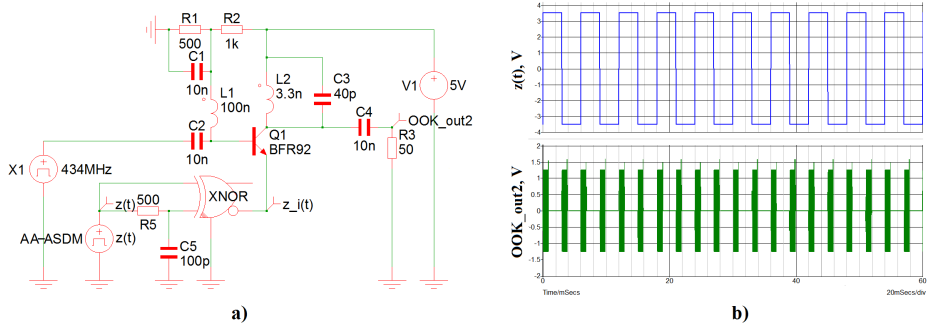


Figure 4.7: Operation of the OOK transmitter: a) electric circuit; b) AA-ASDM2 output signal $z(t)$ and OOK output signal OOK_out2 driven by the output of AA-ASDM2.

In this case, the power consumption of the circuit is directly proportional to the number of AA-ASDM2 switching time instants ($N_{AA-ASDM}$):

$$P_{OOK_{mod}} = P_0(1 - n \cdot \frac{\tau_{tx}}{T_{tx}}) + n \cdot \frac{P_{tx} \cdot \tau_{tx}}{T_{tx}}, \quad (4.1)$$

where P_0 - is an average power consumption of the circuit, when LC is not oscillating, but P_{tx} , when LC is oscillating during and after each transmission; τ_{tx} is a length of the transmitting pulse (including decay time of oscillations), T_{tx} is a period in which the circuit is analyzed, but n is an average number of pulses during T_{tx} .

It follows, if the OOK transmitter is driven by the AA-ASDM2 output, instead of ASDM, there are fewer switching time instants which results in reduced power consumption of the OOK circuit. A comparison of the power consumption of the OOK depending on if ASDM or AA-ASDM2 circuit's output is used as an input for the OOK transmitter is shown in Table 4.3.

Table 4.3: Comparison of the power consumption of the OOK circuit depending on if ASDM or AA-ASDM circuit's output is used as an input for the OOK transmitter

	$C1 = 100nF$	$C1 = 200nF$	$C1 = 400nF$	$C1 = 800nF$
N_{ASDM}	137	69	34	17
P_{ASDM_OOK} (mW)	63.63890	40.52755	28.81639	22.67473
$N_{AA-ASDM}$	69	34	16	10
$P_{AA-ASDM_OOK}$ (mW)	40.34187	28.72533	20.57792	19.02582

As can be seen in Table 4.3, the reduction of the power consumption of the transmitter by using AA-ASDM2, instead of ASDM, can reach up to $\approx 37\%$ depending on the number of switching time instants. But, it is important to note that in this case the power consumption of the circuit when it is not transmitting is very high ≈ 16.6 mW, while modern wireless transmitters have it in a

range of nW. This means, if the power consumption of the circuit, when it is not transmitting, would be for example 100nW, the reduction of the power consumption could reach up to $\approx 50\%$ depending on the number of switching time instants or even more if signals with wide dynamic range is used (see Section 4.1.3), where AA-ASDM2 is particularly advantageous.

Since modern wireless data transmitters consume ≈ 3 mW, it follows that if AA-ASDM2 instead of ASDM is used, it is possible to reduce the power consumption of the transmitter by 1.5 mW, while increasing the power consumption of the encoder just by 4.5 nW, giving a total of $\approx 50\%$ power consumption reduction in a wireless BCI system, leading to two times longer battery life and operation time of wireless system.

4.3 Practical Implementations

Based on the AA-ASDM2 modeling results in Section 4.2.2, a physical AA-ASDM2 based EEG data acquisition system is designed. The block diagram of the designed system is shown in Figure 4.8. It consists of a wireless sensor, which includes EEG signal amplifier, AA-ASDM2 and



Figure 4.8: Full one channel block diagram.

OOK transmitter, and receiving and processing unit, which includes super-heterodyne receiver, ATS460 digitizer and personal computer (PC). Developed AA-ASDM2 based Wireless Sensor for EEG data acquisition and receiver is shown in Fig. 4.9. The working principles of each of

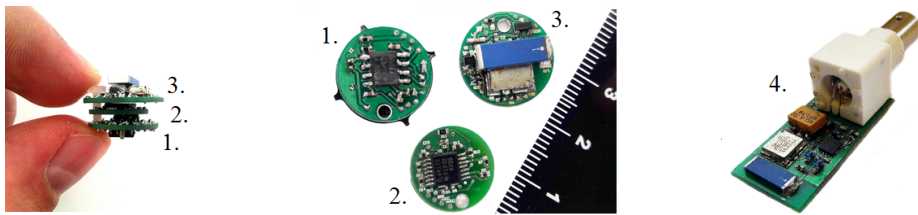


Figure 4.9: Developed AA-ASDM2 based EEG data acquisition system's components: 1. EEG amplifier, 2. AA-ASDM, 3. OOK transmitter, 4. receiver.

the blocks in Fig.4.8 and PCBs in Fig. 4.9 are shown in the full thesis.

In order to test and assess the developed AA-ASDM2 based EEG data acquisition system first AA-ASDM2 is calibrated by analyzing the actual outputs of the AA-ASDM2 PCBs integrator $y(t)$ and trigger $z(t)$ for three different DC input signal voltage levels (in this case, DC=0V, 0.5V and 0.9V). As a results, the actual AA-ASDM2 circuit parameters: $+b$, $-b$, Δt_{\max} and Δt_{\min} are acquired.

In order to verify if developed AA-ASDM2 PCB is working properly, acquired Δt_{\max} and Δt_{\min} values are compared to the theoretically calculated values, where theoretical values are

calculated from the electrical scheme, shown in Fig. 4.10. The ratio of practically acquired

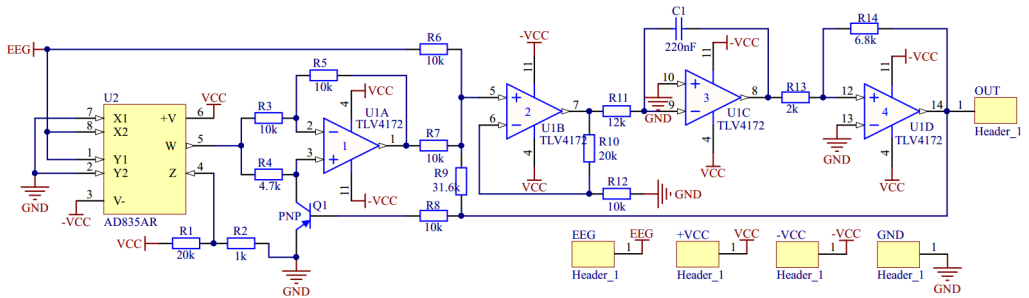


Figure 4.10: AA-ASDM electrical scheme of the actually developed PCB.

values and theoretically calculated must be equal or almost equal. As the calculations show, the difference is within the range of 4 %. This is due to capacitor non-ideality, as it has $\pm 10\%$ capacitance tolerance. As experimental results show, the precision of the reconstruction is very sensitive to capacitor non-ideality and therefore the circuit must be calibrated first. In further experiments, the value of $\frac{1}{f_c}$ is selected based on the practical measurements.

After calibration of the AA-ASDM2 and initial tests, the AA-ASDM2 circuit can be placed in the overall AA-ASDM2 based EEG data acquisition system for further experimental tests. A block diagram of the experimental setup is shown in Fig. 4.11.

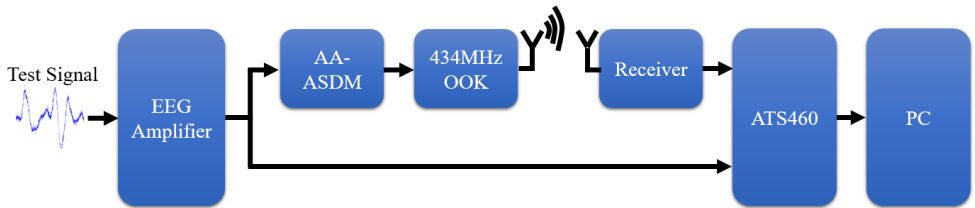


Figure 4.11: Block diagram of the experimental setup.

Knowing the parameters of the AA-ASDM2 circuit, it is possible to acquire, process and reconstruct the original signal.

An example of original and reconstructed signals is given in Fig. 4.12.

As can be seen in Fig. 4.12, it is hard to see the difference between the original and reconstructed signal, which means that it is possible to encode and qualitatively reconstruct the signal, by using AA-ASDM2. In order to quantitatively estimate the performance of AA-ASDM it must be implemented in a chip, with specialized circuit structures with decreased operating supply voltage, capacities, etc., with low comparator jitter, slew rate, DC gain, voltage saturation, excess loop delays and comparator offsets, etc. [25], [38] Also, as shown is [39], Time-to-digital converter (in this case *ATS460*) has a significant impact on the precision of the reconstructed signal. The precision of the reconstructed signal is directly proportional to the t_k measurement precision. [40]

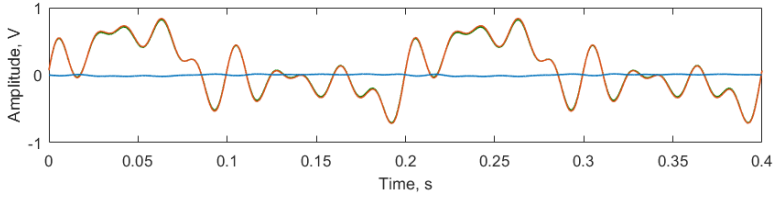


Figure 4.12: Original signal (red line), reconstructed signal (green line) and error signal (blue line), which is the difference between original and reconstructed signal.

4.4 Conclusions

From the simulations, it can be calculated that AA-ASDM1, for different β values, can achieve up to 65.69 % energy saving for transmitter compared to ASDM. Although AA-ASDM1 is advantageous over ASDM in terms of number of samples, it has few drawbacks. For example, there is a need to transmit two signals instead of one and there is a delay introduced by additional envelope signal reconstruction prior to the original signal reconstruction. Even further, the physical implementation of the AA-ASDM1 involves envelope detector which introduce additional delay to the system and synchronization with the original signal. This can be overcome by using AA-ASDM2, where the gain is even bigger and can reach up to 68.85 % less switching time instants compared to ASDM. But this gain comes with more time consuming signal reconstruction due to optimization algorithm. Still, the performance of AA-ASDM2 is admissible, since reconstruction algorithms can reconstruct the signal in real-time on PC. Even further, AA-ASDM2 has lower complexity of the encoding circuit, since it does not involve an additional encoding circuit for the envelope, as it is in AA-ASDM1 case.

From the modeling, it can be concluded that the increased power consumption (by ≈ 60 %) of AA-ASDM2, compared to ASDM, is relatively small (4.5 nW) if compared to the power consumption reduction in the transmitter (by 1.5 mW), which is achieved by having fewer switching time instants at the output of the AA-ASDM2. The average power consumption of presented event-driven OOK circuit decrease proportionally if the number of switching time instants decreases. Using AA-ASDM2 instead of ASDM in wireless BCI system leads to 2 times longer battery life and operation time.

From the practical implementation, it can be concluded that AA-ASDM2 can be used for EEG signal encoding and reconstruction. In order to quantitatively estimate the performance of AA-ASDM it must be implemented in a chip, with specialized circuit structures with decreased operating supply voltage, capacities, etc., with low comparator jitter, slew rate, DC gain, voltage saturation, excess loop delays and comparator offsets, etc. Also, Time-to-digital converter (in this case *ATS460*) has a significant impact on the precision of the reconstructed signal. The precision of the reconstructed signal is directly proportional to the t_k measurement precision.

5. CONCLUSIONS

The main aim of this thesis to develop an improved method for signal encoding based on ASDM, which allows to reduce the power consumption of the wireless BCI system, while maintaining the desired signal quality has been reached.

According to defined tasks, following results are achieved:

- based on the literature review and analysis of electroencephalogram (EEG) signals and brain-computer interface (BCI) systems, the author has defined the requirements for Analog-to-digital converters (ADC). These requirements are: energy efficiency, encoding complexity, resolution and sampling rate;
- based on defined requirements, the author has reviewed, analyzed and described a literature on synchronous and asynchronous ADCs as well as selected the most appropriate ADC for EEG signal encoding and BCI systems as whole; Due to its great properties, Asynchronous Sigma Delta modulator (ASDM) is selected;
- the author has extensively analyzed, researched and described the ASDM and identified the points of improvement. The main inefficiency of the ASDM is related to over-triggering, which occurs when ASDM is applied to wide dynamic range signals such as EEG signals. Due to wide dynamic range that these signals have, a high switching activity of ASDM circuit appears when the input signal amplitude is low;
- in order to improve te ASDM, the author has proposed and in detail described a new method, called Amplitude-Adaptive Asynchronous Sigma-Delta modulator (AA-ASDM), which allows to reduce the over-triggering of the circuit and thus the power consumption of the whole wireless BCI system, while maintaining the desired signal quality;
- in order to test and assess the proposed method, the author has simulated (in *Matlab*), modeled (in *SIMetrix*), designed (in *Altium Designer*) and developed the AA-ASDM. The main achieved results are provided and assessed, and conclusions given;
- the author has developed and tested a complete one channel BCI system. The main achieved results are provided and assessed, and conclusions given.

Based on the results, described above, it can be concluded that the main aim of this work is achieved.

BIBLIOGRAPHY

- [1] M.F. Bear, B.W. Connors, and M.A. Paradiso. *Neuroscience: Exploring the Brain, Third Edition*. Lippincott Williams & Wilkins, 2007, pp. 857, ISBN: 978-0781760034.
- [2] S. Sanei and J.Chambers. *EEG Signal Processing*. Wiley, 2013, pp. 312, ISBN: 978-1118691236.
- [3] I. Iturrate, J. Antelis, and J. Minguez. *Synchronous EEG Brain-Actuated Wheelchair with Automated Navigation*. Robotics and Automation. ICRA '09. IEEE International Conference on, 2009, pp. 2318-2325.
- [4] K. Feong-Hun, F. Biessmann, and L. Seong-Whan. *Reconstruction of Hand Movements from EEG Signals Based on Non-Linear Regression*. Brain-Computer Interface (BCI), International Winter Workshop on, 2014, pp. 1-3.
- [5] R. Rojas, D. Goehring, D. Latotzky, and M. Wang. *Semi-autonomous Car Control Using Brain Computer Interfaces*. Proceedings of the 12th International Conference IAS-12. Advances in Intelligent Systems and Computing, Volume 194., 2013, pp. 393-408.
- [6] M. Renaudin. *Asynchronous Circuits and Systems: a Promising Design Alternative*. in Journal of Microelectronic Engineering, 2000, pp. 133-149.
- [7] A. Yakovlev, D. Kinniment, and B. Gao. *Synchronous and Asynchronous A-D Conversion*. in IEEE Transactions on VLSI Systems, vol.8, 2000, pp. 217-220.
- [8] S. Senay, L.F. Chaparro, S. Mingui, R. Sciabassi, and A. Akan. *Asynchronous Signal Processing for Brain-Computer Interfaces*. Electrical and Electronics Engineering, 2009. ELECO 2009. International Conference on, 2009, pp. II-30-II-35.
- [9] A.A. Deshmukh, R. Deshmukh, and R.Patrikar. *Low Power Asynchronous Sigma-Delta Modulator Using Hysteresis Level Control*. VLSI (ISVLSI), 2011 IEEE Computer Society Annual Symposium on, 2011, pp. 353-354.
- [10] G.D. Colletta, O.O. Dutra, L.H.C. Ferreira, and T.C. Pimenta. *An ultra-low-power first-order asynchronous sigma-delta modulator for biomedical applications*. SOI-3D-Subthreshold Microelectronics Technology Unified Conference (S3S), 2013 IEEE, 2013, pp. 1-2.
- [11] K. Ozols, M. Greitans, and R. Shavelis. *EEG Data Acquisition System Based on Asynchronous Sigma-Delta Modulator*. Electronics Conference (BEC), 2012 13th Biennial Baltic, 2012, pp. 183-186.
- [12] K. Ozols, R. Shavelis, and M. Greitans. *Amplitude adaptive asynchronous sigma-delta modulator*. In *2013 8th International Symposium on Image and Signal Processing and Analysis (ISPA)*, pages 467–470. IEEE, 2013.
- [13] K. Ozols. *Implementation of reception and real-time decoding of asdm encoded and wirelessly transmitted signals*. In *Radioelektronika (RADIOELEKTRONIKA), 2015 25th International Conference*, pages 236–239. IEEE, 2015.

- [14] K. Ozols and R. Shavelis. Amplitude adaptive asdm without envelope encoding. In *2016 24th European Signal Processing Conference (EUSIPCO)*, pages 165–169, 2016.
- [15] D. Lee, J. Yoo, K. Choi, and J. Ghaznavi. Fat tree encoder design for ultra-high speed flash a/d converters. In *Circuits and Systems, 2002. MWSCAS-2002. The 2002 45th Midwest Symposium on*, volume 2, pages II–87. IEEE, 2002.
- [16] Synopsys. Designware 12-bit, 110 msp/s adc. https://www.synopsys.com/dw/doc.php/ds/a/dwc_adc_12b_110mhz_14.pdf?fe=y, 2016. [Online; accessed 17-March-2016].
- [17] E. Delagnes, D. Breton, F. Lugiez, and R. Rahmanifard. A low power multi-channel single ramp adc with up to 3.2 ghz virtual clock. *IEEE Transactions on Nuclear Science*, 54(5):1735–1742, Oct 2007.
- [18] Analog Devices. Low cost, complete 12-bit resolver-to-digital converter. <http://www.analog.com/media/en/technical-documentation/data-sheets/AD2S90.pdf>, 2016. [Online; accessed 17-March-2016].
- [19] T. K. H. Roy and T. H. Teo. A 0.9v 100nw rail-to-rail sar adc for biomedical applications. In *Integrated Circuits, 2007. ISIC '07. International Symposium on*, pages 481–484, Sept 2007.
- [20] F. Cannillo, E. Prefasi, L. Hernández, E. Pun, F. Yazicioglu, and C. Van Hoof. 1.4 v 13 μ w 83db dr $\sigma\delta$ modulator with dual-slope quantizer and pwm dac for biopotential signal acquisition. In *ESSCIRC (ESSCIRC), 2011 Proceedings of the*, pages 267–270. IEEE, 2011.
- [21] L. Zhu, H. Chen, X. Zhang, K. Guo, S. Wang, Y. Wang, W. Pei, and H. Chen. *Design of Portable Multi-Channel EEG Signal Acquisition System*. Biomedical Engineering and Informatics, BMEI '09. 2nd International Conference on, 2009, pp. 1-4.
- [22] R. Elliott. Zero crossing detectors and comparators. <https://www.scribd.com/doc/97388393/Zero-Crossing-Detectors-and-Comparators>, 2016.
- [23] I. Bilinskis. *Digital Alias-free Signal Processing*. UK: Wiley, 2007, pp. 454, ISBN: 978-0470027387.
- [24] E. Allier, G. Sicard, L. Fesquet, and M. Renaudin. A new class of asynchronous a/d converters based on time quantization. In *Asynchronous Circuits and Systems, 2003. Proceedings. Ninth International Symposium on*, pages 196–205. IEEE, 2003.
- [25] S. Ouzounov, E. Roza, H. Hegt, G. Van Der Weide, and A. Van Roermund. An 8mhz, 72 db sfdr asynchronous sigma-delta modulator with 1.5 mw power dissipation. In *VLSI Circuits, 2004. Digest of Technical Papers. 2004 Symposium on*, pages 88–91. IEEE, 2004.
- [26] I. Homjakovs, M. Hashimoto, T. Onoye, and T. Hirose. Signal-dependent analog-to-digital converter based on minimax sampling. In *SoC Design Conference (ISOCC), 2012 International*, pages 120–123. IEEE, 2012.
- [27] A. A. Lazar, E. K. Simonyi, and L. T. Tóth. *Time Encoding of Bandlimited Signals, an Overview*. Electronics Conference (BEC), 2012 13th Biennial Baltic, 2005.

- [28] A.A. Lazar and L.T. Toth. *Time Encoding and Perfect Recovery of Bandlimited Signals*. Acoustics, Speech, and Signal Processing, 2003. Proceedings. (ICASSP '03). 2003 IEEE International Conference on, 2003, vol 6, pp. 709-712.
- [29] S. Senay, L. F. Chaparro, M. Sun, and R. J. Scلابassi. *Adaptive Level-Crossing Sampling and Reconstruction*. 18th European Signal Processing Conference (EUSIPCO-2010), 2010, pp. 1296-1300.
- [30] A.A. Lazar and L.T. Toth. *Perfect Recovery and Sensitivity Analysis of Time Encoded Bandlimited Signals*. IEEE transactions on circuit and systems -I: Regular papers, 2004, vol 51, No. 10 pp. 2060-2073.
- [31] E. Roza. Analog-to-digital conversion via duty-cycle modulation. *IEEE Transactions on Circuits and Systems II: Analog and Digital Signal Processing*, 44(11):907–914, Nov 1997.
- [32] D. Wei and J. G. Harris. *Signal reconstruction from spiking neuron models*. ISCAS (5), 2004, pp. 353-356.
- [33] A.A. Lazar, E.K. Simonyi, and L.T. Toth. *Fast recovery algorithms for time encoded bandlimited signals*. Acoustics, Speech, and Signal Processing, 2005. Proceedings. (ICASSP '05). IEEE International Conference on, 2005. iv/237-iv/240 Vol. 4.
- [34] A. A. Lazar, E. K. Simonyi, and L. T. Toth. *A real-time algorithm for time decoding machines*. Signal Processing Conference (EUSIPCO'2006), 2006 14th European, 2006, pp.1-5.
- [35] M. Renaudin. *Asynchronous circuits and systems: a promising design alternative*. Micro-electronic engineering, 2000, pp. 133-149.
- [36] D. Kinniment, A. Yakovlev, and B. Gao. *Synchronous and asynchronous AD conversion*. Very Large Scale Integration (VLSI) Systems, IEEE Transactions on, 2000, 8.2: pp. 217-220.
- [37] D. Wei, V. Garg, and J. G. Harris. *An asynchronous delta-sigma converter implementation*. Circuits and Systems, 2006. ISCAS 2006. Proceedings. 2006 IEEE International Symposium on, 2006, pp. 4.
- [38] P. Aguirre, V. Camargo, H. Klimach, A. Susin, and C. Prior. Behavioral modeling of continuous-time $\delta\sigma$ modulators in matlab/simulink. In *2013 IEEE 4th Latin American Symposium on Circuits and Systems (LASCAS)*, pages 1–4, Feb 2013.
- [39] A. A. Lazar and L. T. Toth. Perfect recovery and sensitivity analysis of time encoded bandlimited signals. *IEEE Transactions on Circuits and Systems I: Regular Papers*, 51(10):2060–2073, Oct 2004.
- [40] W. Chen and C. Papavassiliou. Asynchronous sigma-delta modulator with noise shaping. *Electronics Letters*, 49(24):1520–1522, November 2013.